11th World Congress on Computational Mechanics (WCCM XI)
5th European Conference on Computational Mechanics (ECCM V)
6th European Conference on Computational Fluid Dynamics (ECFD VI)
E. Oñate, J. Oliver and A. Huerta (Eds)

RUPTURE MECHANISM FOR THIN SHELLS BASED ON ULTRASOUND ACTIVATION FOR SUBCUTANEOUS CONTROLLED DRUG DELIVERY SYSTEMS

SEBASTIÁN CURI[*], DAVID VEYSSET[†§], RONI CANTOR BALAN[†],

STEEVE KOOI[†], KEITH A. NELSON[†§], NOEL M. ELMAN[†] AND

SEBASTIÁN D'HERS[*]

[*] Computational Mechanics Center
Instituto Tecnológico de Buenos Aires (ITBA),
Av. E. Madero 399, Buenos Aires, Argentina, 1106,
Corresponding author: sdhers@itba.edu.ar , www.itba.edu.ar

[†] Institute for Soldier Nanotechnologies
Massachusetts Institute of Technology
, 500 Technology Square, NE47-525, Cambridge, MA 02139
nelman@mit.edu, web.mit.edu/nelman/www

[§] Department of Chemistry
Massachusetts Institute of Technology
77 Massachusetts Avenue, Room 6-235
kanelson@mit.edu , http://nelson.mit.edu/

Key Words: *Dynamic failure, Thin shells, Membranes, Controlled drug delivery, MEMS, Ultrasound.*

Summary: Implantable controlled drug delivery can be used for batch controlled drug release. A novel device for subcutaneous implantation is proposed to eliminate the use of internal electronics and power source, where activation mechanism relies on selectively breaking single reservoirs of an implanted reservoir array using ultrasound.

Laser interferometry is used to determine the deformed shape of the vibrating membrane and estimate the residual stress. Results are used to fit a shell elements model to determine the effective sound pressure on the membrane. With loads, membrane properties and residual stress, energy density criterion is used to analyze failure and modify the design.

Ultrasound induced dynamic failure is shown to be a feasible actuator technology, by tailoring failure conditions using energy density criterion so that the device can be activated at discrete frequencies.

1 INTRODUCTION

Implantable controlled drug delivery devices based on Micro-Electro-Mechanical-Systems (MEMS) have been proposed for a number of clinical applications that require sustained release [1]. Batch controlled release mechanism relies on selectively actuating single reservoirs of an implanted reservoir array as demanded by the pharmacological therapy. Several electro-thermal actuators have been proposed to burst membranes that seal reservoirs, controlled electronically from within the implantable device [2].

A novel device for subcutaneous implantation is proposed to eliminate the use of internal electronics and power source, which uses an external ultrasound source to cause catastrophic failure of the sealing membranes.

Reservoirs are manufactured using Si3N4 Low Pressure Chemical Vacuum Deposition (LPCVD) and subsequent anisotropic silicon etch using KOH. Membranes are supported in a SCS wafer (0.5mm) and exhibit residual stresses (100MPa– 1400MPa) due to the fabrication process [3]. Membrane dimensions are key parameters for single reservoir activation and to ensure hermeticity prior to activation. Lateral dimensions are in the 250µm-1mm range and thickness is in the 50nm-250nm range.

The paper is organized as follows. To explore membrane failing conditions, manufacturing membrane residual stress has to be estimated. For this purpose the 1st resonant frequency is experimentally measured through an indirect method (Section 2). With the residual stress estimation at hand, the deformation caused by ultrasound is measured and correlated with a numerical finite element shell model to obtain an equivalent sound pressure (Uniform pressure that causes same deformation) (Section 3). With the membrane stress and the equivalent sound pressure, energy density failure criterion is applied and membrane design is modified to cause catastrophic failure (Section 4).

2 EXPERIMENTAL SETUP

2.1 Optical observation of a vibrating membrane

Different membranes were imaged while being acoustically excited by a commercial speaker in order to characterize their vibrational modes and frequency response. By spanning the excitation frequency in the [1 kHz – 100 kHz] range, we were able to determine frequencies where the membrane experienced resonant like deformation with an associated vibration amplitude.

The membrane is imaged onto a CCD camera using a femtosecond laser (λ_{laser} = 400 nm, 150 femtoseconds duration) pulse, derived from a Ti:Sapphire amplifier, and a simple two-lens configuration (Figure 1). An interferometric image (Figure 2) is obtained using a reference beam - derived from the same amplified laser pulse - through a classical Michelson interferometer (Figure 1). Since the oscillation period of the membrane is large compared to the laser pulse duration, the phase of the speaker excitation signal needs to be adjusted manually with a delay generator so that the membrane is imaged at its maximum deviation. Each fringe jump, e.g. black fringe to black fringe, represents an optical path length difference of λ_{laser}, therefore a height difference (or deviation) of $\lambda_{laser}/2$ of the membrane surface (as in reflection configuration). The surface contour of the membrane is extracted directly from the recorded image.

For all the tested membranes, the only observed mode shape was the 1st vibrational mode shape at several frequencies with varying amplitude. Higher modes were not observed. This set of results can be attributed to harmonic distortion in the speaker system. It is known that speakers experience harmonic distortion [4], which is the appearance of an infinite amount of higher exciting frequencies spaced among each other the fundamental one. This means that when the input of a speaker has f frequency, output will have a frequency spectrum with f, 2f, 3f, … peak frequencies, and each of those peaks with variable amplitude depending on speaker non-linearity. This hypothesis is applied in next section to estimate the 1st vibrational mode frequency.

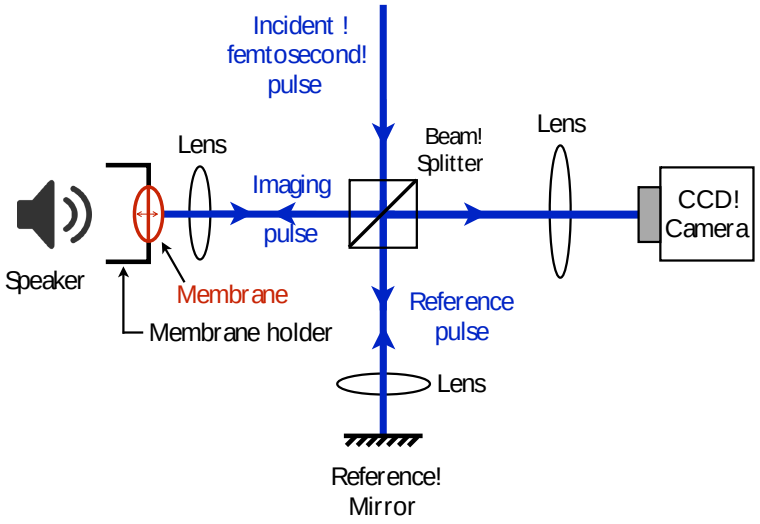

Figure 1: The membrane is acoustically excited with a speaker disposed few centimeters away and is imaged on the CCD camera using a femtosecond pulse. The speaker is driven with a sinusoidal signal whose frequency is tuned manually. The interference of the beams reflected from the vibrating membrane and a reference mirror gives rise to an interferometric image on the CCD.

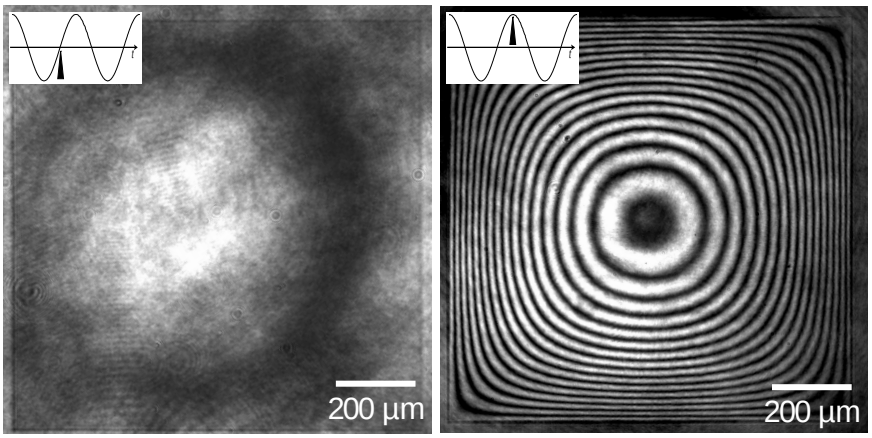

Figure 2: Interferometric images of a vibrating 1 mm^2 membrane at its resonance frequency of 20.2 kHz. (Left) The image was captured when the membrane shows almost zero deflection during its vibration. (Right) The relative phase of the speaker was adjusted relatively to the laser time of arrival so that the membrane is imaged at its maximum deviation characterized by a maximum number of fringes. The interferometric image is a direct representation of the contour of the membrane surface. (Inset) The black arrows indicate the time at which the membrane is imaged in the course its oscillations.

These measurements are extremely informative quantitatively but not practical for systematic characterization. For each frequency, the signal phase has to be manually adjusted as explained earlier, making it cumbersome to cover the entire range continuously. However, once it is established that the only excited vibrational mode is the 1st mode, measuring the amplitude of vibration versus excitation frequency is sufficient to determine the response spectrum. To do so in the future, we are planning to implement a complementary setup similar to [5] commonly used to detect surface acoustic waves. This technique, based on cw-laser probe beam deflection, would enable fast and complete measurements of different membranes' frequency response.

2.2 Resonant Frequency Estimation

Focusing on the 1µm side membrane, 1^{st} vibrational mode was obtained when the speaker was set at several frequencies, see Table 1.

Table 1: Speaker frequencies that excite 1^{st} vibrational mode for 1µm square membrane and 50 nm thickness.

4.3 kHz
8.3 kHz
17.0 kHz
20.2 kHz
23.7 kHz
26.3 kHz

4.3 kHz
8.3 kHz
17.0 kHz
27.2 kHz

Using these measured frequencies, we search the spectrum for the frequency f_1 that minimizes the sum of squared difference to integer product of f_1,

$$e_f = \sqrt{\frac{1}{m}\sum_{1}^{m} min\left(ceil\left(\frac{f_m}{f_1}\right) - \left(\frac{f_m}{f_1}\right), \left(\frac{f_m}{f_1}\right) - floor\left(\frac{f_m}{f_1}\right)\right)^2} \quad (1)$$

being e_f the relative error for each target frequency and m the number of measured frequencies. In Figure 3 e_f distribution is plotted. The range adopted is 50 to 450 KHz according to residual stresseses found in literature [3] and their corresponding natural frequencies. The f_1 that minimizes it is hence considered to be the 1st vibration resonant frequency, 241 kHz.

Although this result is theoretically feasible, the fact that is the 56th harmonic distortion of 4.3kHz frequency calls authors attention. Further experimental validation is required.

The residual stress can be obtained from [6]

$$f_1 = \frac{1}{2l}\sqrt{2\frac{\sigma_r}{\rho}} \quad (2)$$

where, l is the membrane lateral dimension (1 µm), σ_r the residual stress and ρ the density (2900kg/m^3). Hence $\sigma_r = 337$MPa.

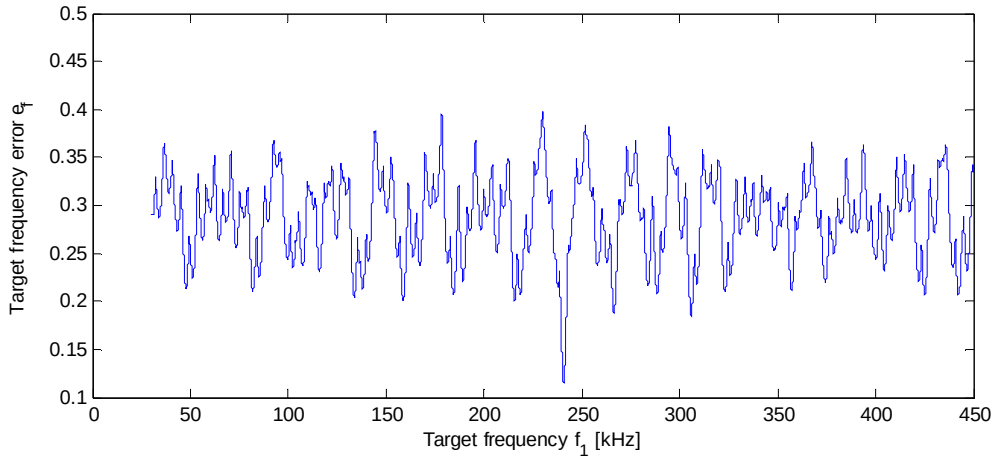

Figure 3: Target frequency error e_f for 1µm square membrane and 50 nm thickness.

3 NUMERICAL MODEL

3.1 Shell Model

From structural point of view, membranes are thin shells with axial and bending stiffness. The 4 node shell element with Mixed Interpolation of Tensorial Components (MITC-4) [7] under Reissner-Midlin hypothesis is adopted for the finite element model. The manufacture residual stress obtained in section 2.2 is introduced into thin shell dynamic through the stress stiffening matrix [8].

Regarding boundary conditions, clamped and simply supported conditions are tested and compared to interferometry analysis results. It is found that best fit is found when boundaries are simply supported and not clamped. This means that the support wafer is not capable of restricting rotations on the membrane.

3.2 Equivalent Sound Pressure

Residual stress estimation and the deformed shape of the vibrating membrane obtained from laser interferometry are used to determine the Equivalent Sound Pressure in order to understand the loads the membrane undergoes. The image is filtered and mid-side and diagonal deflection profiles are obtained and compared to the Shell Model developed in section 3.1.

The pressure is calibrated adjusting maximum membrane displacement and shape heuristically. In Figure 4 the calibration is shown for the 20.2 kHz excitation case. Equivalent Sound Pressures obtained for other excitation frequencies are shown in Figure 5.

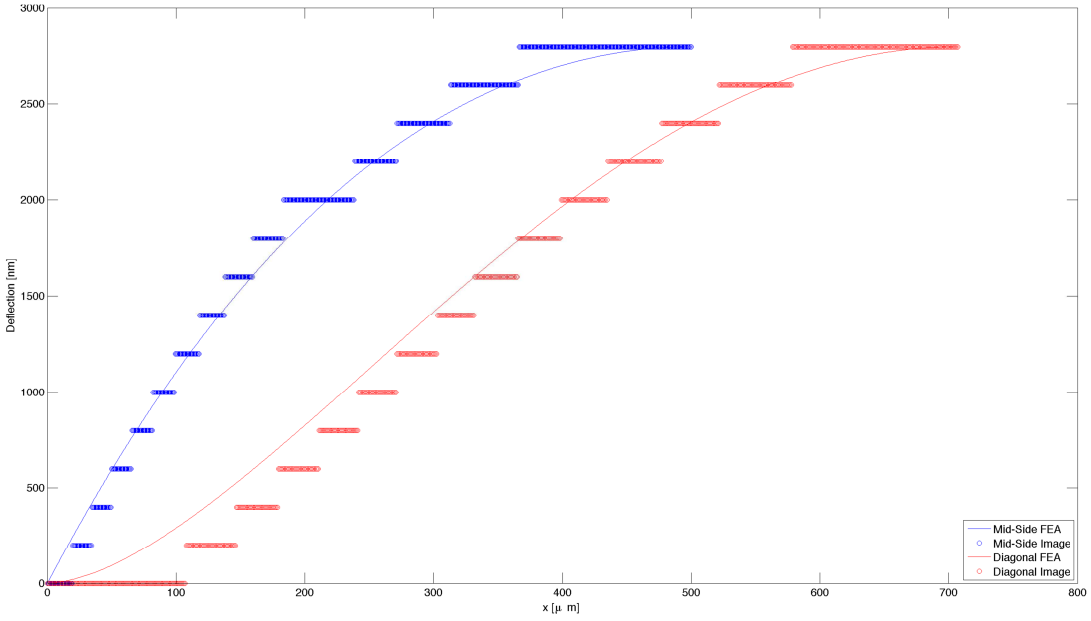

Figure 4: Adjusted shape for 20.2 kHz excitation 1μm square membrane and 50 nm thickness.

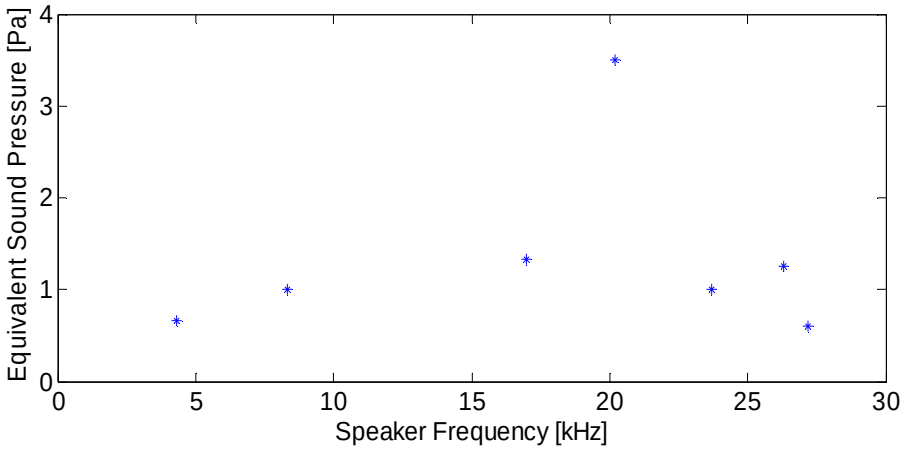

Figure 5: Obtained Equivalent Sound Pressures for 1µm side membrane and 50 nm thickness.

4 FAILURE

4.1 Failure Criterion

Since during experiments no membrane failure was observed, regardless of size and thickness ratios and the power involved, Energy density criterion is adopted to understand failure threshold and to be used later as design tool. It was chosen due to the Si_3N_4 brittleness and the dynamic loading conditions of the problem under study [9].

Several membrane modifications and mass additions are tested to finally find that rupture can be reached by local addition of nonstructural mass to the membrane at one corner. This added mass prevents membrane from moving and concentrates Energy density. See Figure 6 for the Energy density plots and a photograph of a membrane with the nonstructural mass added. Energy density threshold value is yet to be determined since only failure, non-failure results could be obtained.

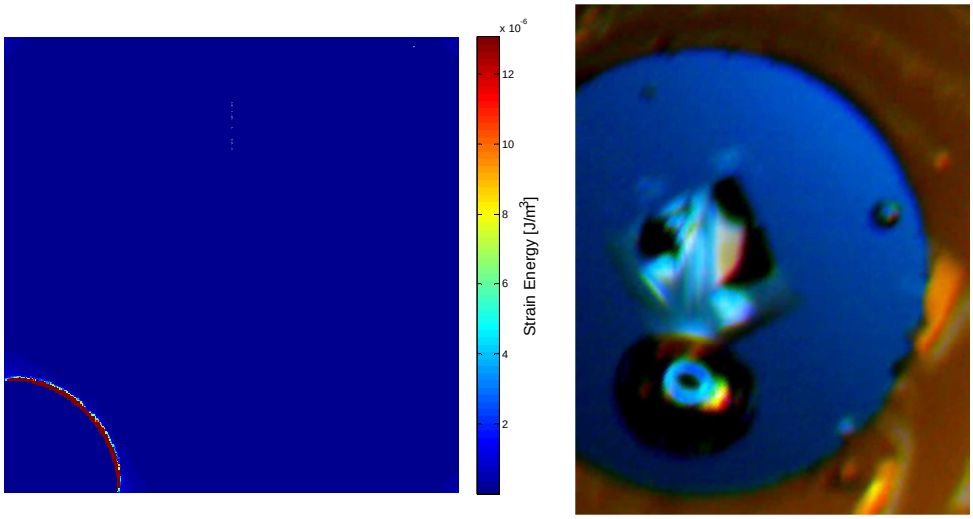

Figure 6: Energy density pattern and photograph for 1µm square and 50 nm thickness membrane with added mass.

5 CONCLUSIONS AND FUTURE WORK

Ultrasound induced dynamic failure is a feasible actuator technology to be used in micro-devices. Concept has been simulated, manufactured and tested.

Further understanding of the speaker as bursting device, particularly the selectivity that can be reached when harmonic distortion is present is necessary to be able to burst individual membranes without risking bursting other membranes in the array.

In order to characterize membrane mechanical behavior a method based on harmonic distortion was developed, however a more reliable membrane residual stresses measurement technique must be applied.

Since thin shells mechanics can be accurately reproduced, future work will focus on tailoring failure conditions using modal energy density so that the device independent reservoirs can be activated at discrete frequencies.

ACKNOWLEGDEMENTS

This research work was supported by the US Army Research Office via the Institute for Soldier Nanotechnologies (ISN) at MIT (contract: W911NF-07-D-0004) in collaboration with Instituto Tecnológico de Buenos Aires.

REFERENCES

[1] Elman N.M. and Upadhyay U.M., Medical Applications of Implantable Drug Delivery Microdevices Based on MEMS (Micro-Electro-Mechanical-Systems), . *Current Pharmaceutical Biotechnology*, (2010) **11:**398-403.

[2] Elman N.M., Masi B.C., Cima M.J and Langer R., Electro-thermally induced structural

failure actuator (ETISFA) for implantable controlled drug delivery devices based on micro-electro-mechanical-systems. *Lab Chip* (2010) **10(20)**:2796-804.

[3] Noskov A.G., Gorokhov E.B., Sokolova G.A., Trukhanov E.M. and Stenin S.I., Correlation between stress and structure in chemically vapour deposited silicon nitride films. *Thin Solid Films* (1988) **162**:129-143.

[4] Sturtzer E., Pillonnet G., Lemarquand G. and Abouchi N., Comparison between voltage and current driving methods of a micro-speaker, *Applied Acoustics*, (2012) **73**(11):1087-1098.

[5] Bennis A., Lomonosov A.M., Shen Z.H. and Hess P., Laser-based measurement of elastic and mechanical properties of layered polycrystalline silicon structures with projection masks. *Applied Physics Letters* (2006) **88**:101915.

[6] Jöckel A., Rakher M.T., Korppi M., Camerer S., Hunger D., Mader M. and Treutlein P., Spectroscopy of mechanical dissipation in micro-mechanical membranes, Appl. Phys. Lett. (2011) **99**:143109

[7] Dvorkin E. N. and Bathe K. J., A continuum mechanics based four-node shell element for general non-linear analysis, *Engineering Computations* (1984) **1(1)**:77–88.

[8] Hinton E., Bićanić N., A comparison of Lagrangian and serendipity Mindlin plate elements for free vibration analysis, *Computers & Structures* (1979) **10(3)**:483-493.

[9] Yu T.X. and Chen F.L., Failure of plastic structures under intense dynamic loading: modes, criteria and thresholds, *International Journal of Mechanical Sciences* (2000) **42(8)**:1537–1554.